Morphology–Property Relationships in ABS/PET Blends. I. Compositional Effects

WAYNE D. COOK,[1,*] TIE ZHANG,[2] GRAEME MOAD,[3] GARY VAN DEIPEN,[3] FERENC CSER,[2] BRONWYN FOX,[2] and MICHAEL O'SHEA[2]

[1]Department of Materials Engineering, Monash University, Clayton, Vic, Australia 3168, [2]CRC for Polymer Blends, 32 Business Park Drive, Notting Hill, Vic, Australia 3168, and [3]CSIRO Division of Chemicals and Polymers, Private Bag 10, Rosebank MDC, Vic, Australia 3169

SYNOPSIS

Novel blends of PET and ABS were prepared by extrusion and injection molding. DSC and DMTA studies show that PET and ABS are immiscible and that the blends consist of four phases: SAN, grafted polybutadiene, amorphous PET, and minor amounts of crystalline PET. The morphology was investigated by transmission electron microscopy on OsO_4-stained and unstained sections and by scanning electron microscopy of alkali- and solvent-etched surfaces. These techniques reveal that the two major domains, SAN and amorphous PET, interpenetrate and are cocontinuous over the compositional range of 30–70 wt % PET. The yield stress and flexural modulus increase in an almost linear fashion as the weight fraction of PET in the blend is increased. In contrast, the notched Izod impact energy passes through a maximum and the Dart impact energy shows a step transition at 50 wt % PET. SEM studies of the Izod fracture surfaces exhibit considerable plastic deformation in both domains when the specimens are tough, indicating that both phases participate in the toughening process. © 1996 John Wiley & Sons, Inc.

INTRODUCTION

The blending of two dissimilar polymers offers the potential of providing a material with the advantages of each and at a fraction of the research costs normally associated with the synthesis of new polymer systems. In general, the polymers are selected on the basis of the particular properties that they may offer in the blended state such as toughness, chemical resistance, or heat stability. However, the rule of mixtures (which predicts that blend properties will be the average of their ingredients) generally does not hold in polymer blends because the blend components are usually not totally miscible and form a two-phase structure.[1]

Conventional wisdom in blending immiscible polymers states that optimum blend properties are obtained by the use of a compatibilizing agent which has two or more segments which are miscible with one of the two blend phases but not with both. These compatibilizers are believed to function by reducing the interfacial energy[1] and stabilizing the domain structure. In some circumstances, this may also lead to the development of a cocontinuous structure in which each phase interpenetrates the other and such a morphology may provide valuable properties. The compatibilizer may also improve adhesion between the domains and aid stress transfer between them. For some systems, such as ABS (acrylonitrile–styrene–butadiene copolymer)/polycarbonate (PC) blends, no compatibilizer is required for stable morphology and high strength,[2,3] possibly due to the partial miscibility of the phases.[3]

In the present work, engineering blends were formed between the tough nonpolar thermoplastic styrenic polymer, ABS, and an oil-resistant, polar semicrystalline polyester, poly(ethylene terephthalate) (PET). With the potential of combining chemical polarity, crystallinity, and toughening phases, these new blends not only offer a range of very useful properties but also present a scientific challenge associated with the potential coexistence of four dis-

* To whom correspondence should be addressed.

Journal of Applied Polymer Science, Vol. 62, 1699–1708 (1996)
 CCC 0021-8995/96/101699-10

crete phases in the solid state. The ABS/PET blend may also be commercially significant, especially if it can be formed from recycled materials (such as recycled PET soft drink bottles) and it could replace the more expensive ABS/polycarbonate (PC) blends used in automotive applications. While there are several patents (e.g., see refs. 4–6) on ABS/PET blends, there do not appear to be any reports on this material in the open literature.

EXPERIMENTAL

Table I lists compositional details of the emulsion-polymerized grades of ABS and the PET used in the study. As received, the PET had a number-average molecular weight of 24,500 g/mol (ref. 7) and a degree of crystallinity of approximately 30%.

The PET and ABS were dried at 177°C/4 h and 80°C/16 h, respectively, to minimize PET hydrolysis during processing. All blending was performed at 230–240°C and 100 rpm on a Werner and Pfleiderer ZSK-25 intermeshing, corotating twin-screw extruder with 25 mm-diameter screws, a channel depth of 4.17 mm, an L/D ratio of 45, and with three 4 mm strand dies. After pelletizing the extrudate and drying the blend at 100°C/12 h, all specimens were prepared on an Engel SE600-125 120 tonne reciprocating screw injection molder operated at a screw speed of 40 rpm. The melt temperature was kept at 250°C and the standard molding temperature and cycle time was 60°C and 33 s. In some cases, the mold temperature was varied to study its influence on PET crystallization. Other work has shown[7,8] that the PET in the blend can be degraded during processing. To ensure that the trends presented in the present work were not affected by variation in the molecular weight of the PET in the blend, the PET M_n in the molded blend was determined by a gel permeation technique discussed elsewhere.[7] The average M_n of the PET in the blend was found to be 22,000 ± 1540 g/mol and so the effect of variations in M_n can be ignored.[8]

Type 1 tensile dumbbell specimens were prepared according to ASTM 638-89 with a thickness of 3.2 mm and width of 13 mm. The measurement of tensile yield and breaking stresses and the elongation to break was performed on a Instron 4505 tensile testing machine at 22°C using a crosshead speed of 10 mm/min. The modulus and yield stress were also measured in flexure at 1 mm/min on the gauge section of these specimens in three-point loading (ASTM D790-86) using a span of 51 mm. Notched impact testing was performed with a Zwick (Model 7900) impact tester according to ASTM D256-88 using the gauge section of the tensile specimen. Falling dart impact testing was performed using a Radmada instrumented impact tester operating at a dart speed of ca. 4 m/s. The specimens were 125 × 75 × 3.2 mm molded plaques and the test geometry was similar to the noninstrumented ASTM D3029-84 method and used a hemispherical impacting tup of 6.35 mm radius but utilized a 50 mm-diameter supporting ring (instead of a 38.1 mm diameter as specified for Geometry FB in the Standard).

The thermal properties of the blends were measured by differential scanning calorimetry (DSC) at 10°C/min with a Perkin-Elmer DSC7 on 10 mg samples. The calibration of the DSC was performed with indium and zinc standards. Dynamic mechanical thermal analysis (DMTA) of the blends was performed with double cantilever geometry using a Polymer Laboratories Mk IV DMTA operated at 1 Hz.

Table I Materials Used

Code	Composition	Supplier
ABS1	Acrylonitrile/butadiene/styrene = 25 : 30 : 45 wt %, 42% grafted gel, M_n (ungrafted SAN) = 40,000 g/mol	Huntsman Chemical Co., Australia
ABS2	Acrylonitrile/butadiene/styrene = 19 : 36 : 45 wt %, 69% grafted gel, M_n (ungrafted SAN) = 35,000 g/mol	Hunstman Chemical Co., Australia
PET	Equimolar copolymer of terephthalic acid and ethylene glycol copolymerized with several percent of cyclohexane dimethanol and trace levels of diethylene glycol, M_n = 24,500 g/mol (as received), intrinsic viscosity = 0.95 dL/g	Eastman Chemical Products, Inc.

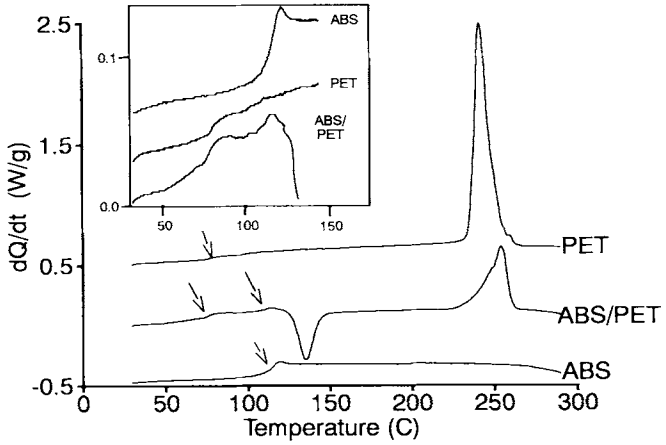

Figure 1 DSC traces of PET, ABS1, and the 50/50 blend. The arrows indicate the heat-capacity steps associated with the glass transitions.

Transmission electron microscopy was performed with a Philips CM20 TEM using a 200 kV accelerating voltage. Thin sections of polymer (100 nm thick) were cut with a diamond knife on a cryo-ultramicrotome (Reichert Ultracut-S) at −90°C. In most cases, the sections were exposed to OsO_4 vapor to stain the polybutadiene (PBD) particles in the micrographs. Micrographs were also taken of the unstained sections.

Scanning electron micrographs of the blends were obtained with a JEOL JSM-840A SEM. Sample surfaces were prepared from freeze-fractured molded plaques as well as from the fractured Izod specimens. The topological structure of the blends was exposed by two alternative selective etching techniques. Since PET is readily hydrolyzed by potassium hydroxide (KOH) whereas ABS is not affected, the ABS morphology was obtained by etching the surface PET with a 10 wt % solution of KOH in ethanol at room temperature, followed by careful washing of the surface with water. SEM studies of the extent of etching of the surface showed only partial etching of the surface after 5 h but virtually identical etching for 15 and 20 h and so a 20 h etch time was used as the standard. Since SAN is soluble in methyl ethyl ketone (MEK) whereas PET is not, MEK was used to etch the ABS domain at room temperature for 15 min in an ultrasonic bath. After room-temperature drying of the surface under vacuum, the specimens were coated with ca. 0.1 μm layer of Au in a Dynavac sputter coater SC150 gold vacuum splattering unit and were examined at ×1000 and ×4000 magnification.

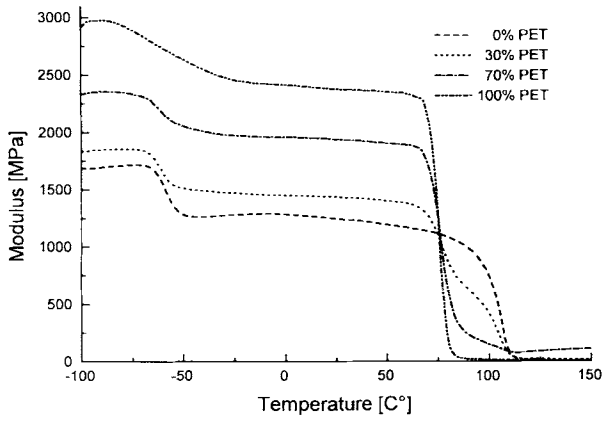

Figure 2 Storage flexural modulus vs. temperature for blends of ABS2 with PET. No corrections were applied for specimen clamping effects, and as a result, the absolute magnitude of the modulus is only approximate.

RESULTS AND DISCUSSION

Structure and Morphology

The DSC trace of an extruded sample of the 50/50 wt % blend of ABS1 with PET is illustrated in Figure 1. A step is evident in the heat capacity near 80°C, which may be attributed to the T_g of the amorphous polyester phase.[9] Another poorly defined heat-capacity step near 110°C can be assigned to the T_g of the SAN domain from the ABS.[10-13] The 110°C transition appears to be overlapped with a PET recrystallization exotherm near 135°C because a similar exotherm (although at a higher temperature of 190°C) was observed in DSC runs of melt-quenched PET. Finally, there is an endotherm at approximately 240°C which is consistent with the melting of crystallites in PET. The energy absorbed in the

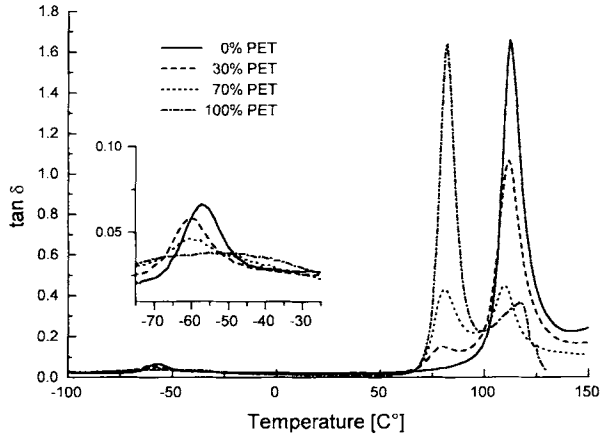

Figure 3 tan δ vs. temperature for blends of ABS2 with PET.

endotherm at 250°C and the energy evolved in the exotherm at 135°C of the blend in Figure 1 are of similar magnitude, suggesting that the PET domain is primarily amorphous in the extruded samples. It has been suggested that in the related blends of ABS/PC[10,14] and SAN (styrene–acrylonitrile)/PC,[10] evidence for partial miscibility can be obtained from shifts of the T_g's compared with the pure components. The application of such an analysis to the ABS/PET blends is complicated by the close proximity of the PET and SAN T_g's and the PET recrystallization exotherm.

The storage flexural modulus and damping factor (tan δ) of molded ABS2/PET blends are shown in Figures 2 and 3 as a function of temperature. Pure PET shows a broad, low-temperature dispersion

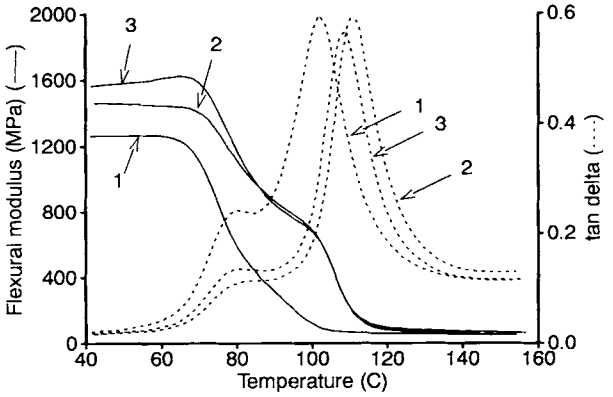

Figure 4 Storage flexural modulus and tan δ vs. temperature for ABS1/PET molded at (1) 60°C/30 s or (2) 80°C/110 s or (3) containing 1% pyrolytic SiO_2 as a nucleating agent. No corrections were applied for specimen clamping effects, and as a result, the absolute magnitude of the modulus is only approximate.

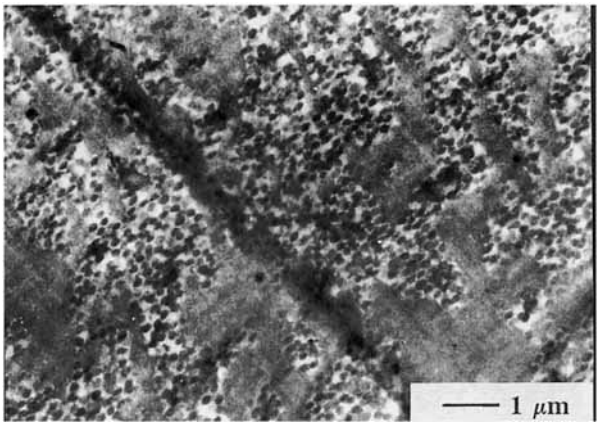

Figure 5 TEM micrograph of OsO_4-stained 50/50 ABS2/PET blends sectioned perpendicular to the flow direction. The dark particles are OsO_4-stained PBD, the surrounding light regions are SAN, and the gray phase is PET.

centered around −60°C due to the β relaxation[9] and a major relaxation near 80°C due to the glass (α) transition.[9] The pure ABS2 sample exhibits a tan δ peak at 113°C due to the glass transition of the SAN phase and a peak at −57°C due to the T_g of the PBD particles. The latter value is considerably higher than the T_g of −78°C reported for emulsion polymerized PBD[15] and it is also greater than that measured for ABS1 (−73°C). These differences might appear to be associated with the grafting to the PBD because, as shown in Table I, ABS1 has a low ratio of grafted SAN to PBD (0.4) while ABS2 has a much higher level (0.92). In support of this suggestion, Kim and Shin[12] found that when SAN is blended

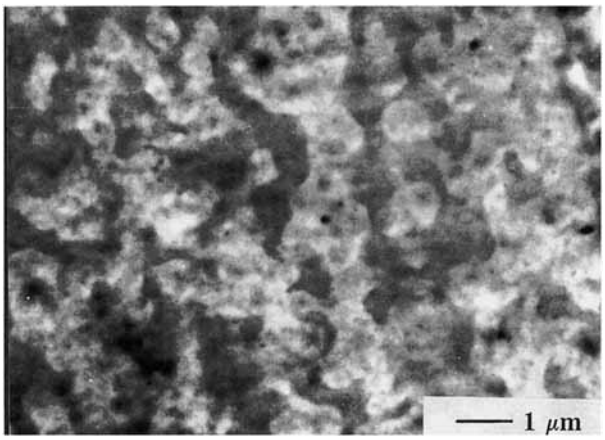

Figure 6 TEM micrograph of unstained 50/50 ABS2/PET blends sectioned perpendicular to the flow direction. The light areas are SAN and PBD while the darker regions are the more electron-dense PET.

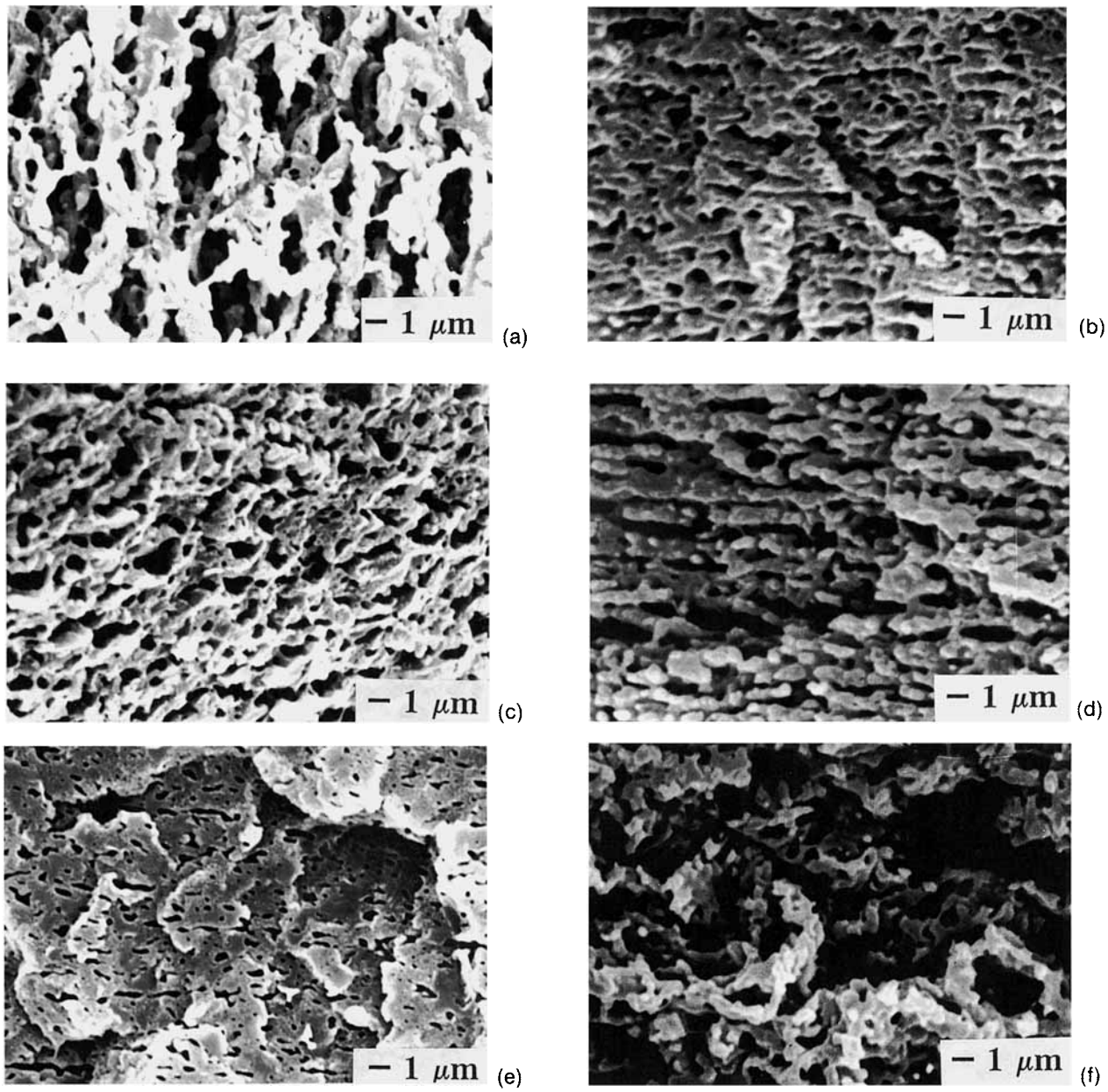

Figure 7 SEM micrographs of freeze-fractured surfaces ABS2/PET blends of wt % compositions: (a, b) 30/70; (c, d) 50/50; (e, f) 70/30. The ABS domain is revealed by selective etching with KOH/ethanol in (a, c, e) while in (b, d, f), the PET domain revealed by MEK etching. The surfaces are perpendicular to the flow direction during molding.

with ABS the T_g of PBD decreases as the fraction of grafted rubber in the sample is diluted with SAN while the SAN T_g is unaffected. However, these conclusions are not consistent with the results of Ricco et al.[11] which showed that as the grafting level in ABS is increased (at constant rubber content) the T_g of the PBD phase decreases. For the present materials, the DMTA T_g of the SAN phase is virtually independent of the rubber content (111°C for ABS1 vs. 112°C for ABS2).

The dynamic mechanical spectra of the blends (Figs. 2 and 3) show transitions in the modulus curves and maxima in the tan δ curves which correspond to the glass transitions for the SAN and PET phases of the parent polymers. As the fraction of PET is increased in the blend, the maximum in

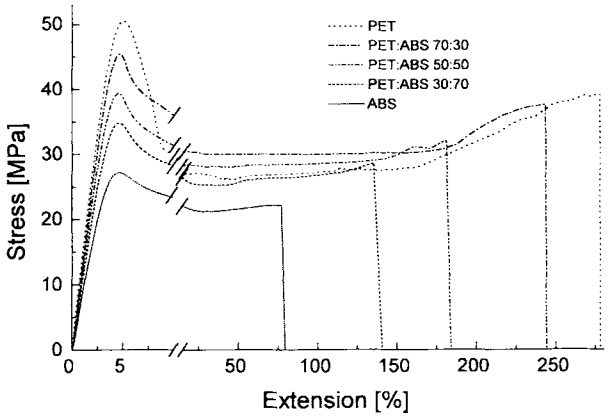

Figure 8 Tensile stress (nominal) vs. % elongation for 0/100, 30/70, 50/50, 70/30, and 100/0 wt % blends of ABS2/PET.

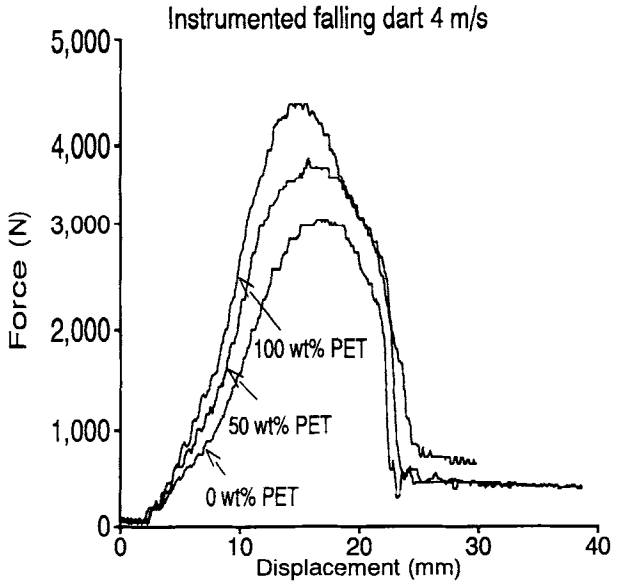

Figure 10 Falling dart impact traces for 0/100, 50/50, and 100/0 wt % blends of ABS2/PET.

tan δ at ca. 80°C due to the PET glass transition increases while the damping due to the ABS component at ca. 110°C is reduced in magnitude. Similarly, the transition due to the polybutadiene at −57°C decreases in magnitude as the wt % PET is increased. These results are analogous to that found in blends of SAN with PC[16] and confirm the presence of separate PBD, SAN, and PET phases. In addition, the T_g's of the PBD and of the SAN phases and of the PET phase were virtually unaffected (<3°C) by blending with PET, suggesting that the PET and SAN have very low miscibility. In contrast, Herpels and Mascia[13] found that for ABS/PC blends both the SAN and PBD glass transitions were shifted by up to 10°C on blending with PC, suggesting that limited miscibility of PC occurred not only in the SAN phase but also on the surface layers of the rubber.

DMTA traces are shown in Figure 4 for a 50/50 blend of ABS1/PET molded at 60°C for 33 s and for a similar specimen which had been molded at a higher temperature (80°C) and for a longer period (110 s). Also shown in the figure is the DMTA trace of a similar blend containing 1 wt % SiO_2. In the latter two curves, the tan δ peak at 80°C due to the T_g of the PET is considerably reduced, suggesting that the samples have undergone increased crystallization due to the higher temperature and longer

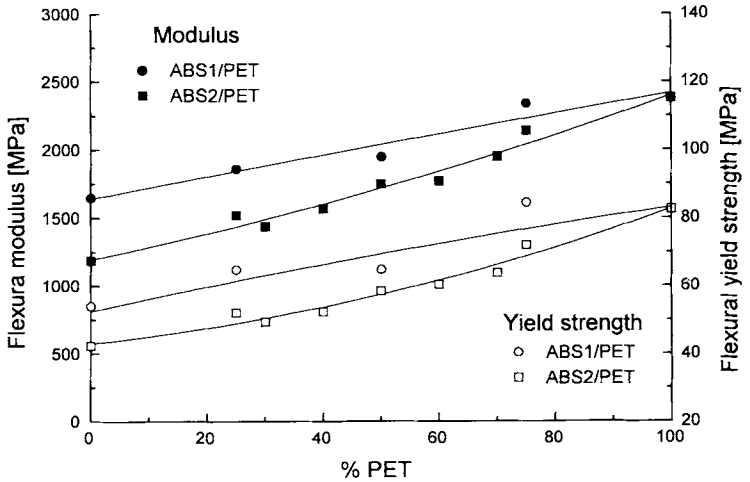

Figure 9 Flexural modulus and yield stress vs. composition in ABS1/PET and ABS2/PET blends.

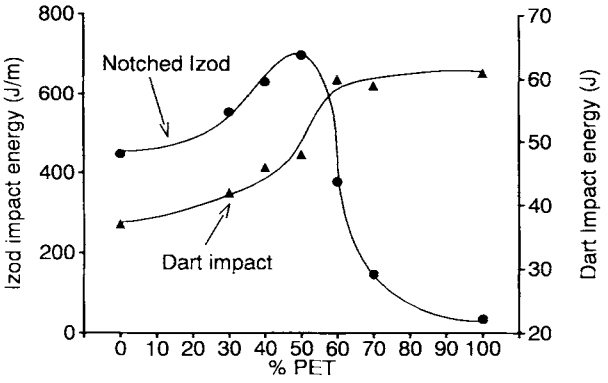

Figure 11 Izod (notched) impact energy and dart impact energy vs. composition in ABS2/PET.

time in the mold or due to the nucleating affect of the SiO_2, thus reducing the fraction of amorphous material in the PET domain.

TEMs of low-temperature microtomed samples from molded 50/50 wt % blends of ABS2 and PET are shown in Figures 5 and 6. In Figure 5, the PBD vinyl groups were stained by OsO_4 and, due to the high electron density of the osmium, the PBD is revealed as dispersed spherical particles, 0.10–0.20 μm in diameter. The light-shaded material surrounding each particle may be identified as SAN because it is the least dense phase and so has the lowest electron density. This SAN phase appears to be continuous throughout the sample and is interpenetrated by another slightly darker domain. Because PET is denser than is SAN, the second continuous phase can be identified as PET. A TEM micrograph of the unstained blend is shown in Figure 6. In this case, PET has the highest electron density and so can be identified as the darker regions while the ABS occurs in the lighter regions. As found in Figure 5, the domains are extended and are of irregular shape, suggesting that the ABS and PET domains are cocontinuous with the other component.

Scanning electron micrographs of selectively etched freeze-fractured molded plaques of ABS2/PET blends are shown in Figure 7. In Figure 7(a, c, e) the PET component of the specimen surface was etched by KOH/ethanol, while for the micrographs shown in Figure 7 (b, d, f) the ABS domain was etched from the surface with MEK. For the 50/50 wt % composition, the ABS [Fig. 7(c)] and PET [Fig. 7(d)] morphologies appear to be continuous throughout the structure, in agreement with that shown by TEM (Figs. 4 and 5). Freeze-fractured surfaces in the other two mutually orthogonal directions revealed a similar microstructure which confirms its cocontinuity. A similar interpenetrating structure was found for the ABS1/PET blend. Since each pair of micrographs represents the microstructure remaining after the other domain was selectively removed, the micrographs should be inversions of one another. For the 50/50 ABS2/PET blend, the size and shape of the holes revealed by one etchant correspond well with the protruding morphology revealed by the opposite etch technique. In Figure 7, the 70/30 and 30/70 wt % blends also show evidence of a cocontinuous structure but with some tendency toward a dispersion of the minor component in the matrix phase. In the ABS2/PET blend with the 30/70 composition, etching of the minor ABS domain also produces a micrograph showing connected holes while etching of the major component (PET) produces an inversion of the microstructure with a lumpy lattice structure protruding from the surface. The ABS microstructure revealed by KOH etching of the PET domain in the 30/70 ABS2/PET blend shows a well-defined porous structure; however, the reverse PET microstructure obtained by MEK etching of the ABS appears distorted. This poorer correlation in the microstructure may be due to the effect of the solvent mixture in swelling the PBD particles and thus distorting the surrounding PET structure.

The micrographs shown in Figure 7 are very similar to those obtained in a number of studies on KOH-etched ABS/PC[14,17,18] and SAN/PC[19] surfaces. In these studies, blends with compositions between 50 and 65 wt % PC were definitely cocontinuous[14,17,18] with some evidence for cocontinuity over a the wider range of 40–70 wt % PC.[17,19]

Fracture Behavior

Figure 8 depicts the stress–strain behavior of ABS2/PET blends. In all cases, ductile behavior is observed, and as the wt % PET is increased, the yield stress, modulus, and breaking strain increases. In Figure 9, the flexural yield stress and modulus are plotted as a function of composition in ABS1/PET and ABS2/PET blends. The modulus of the ABS2 blends are lower than those for ABS1 blends due to the higher rubber content which enhances the flexibility of the ABS component. The higher concentration of rubbery particles in ABS2 also appears to enhance yielding by reducing the triaxiality of the stress state in the matrix surrounding the rubber particles.[20] The tensile yield stress was approximately 63% of the flexural yield stress, which is close to the theoretical factor of $\frac{2}{3}$.[21] The yield stress and modulus are almost linear functions of the compo-

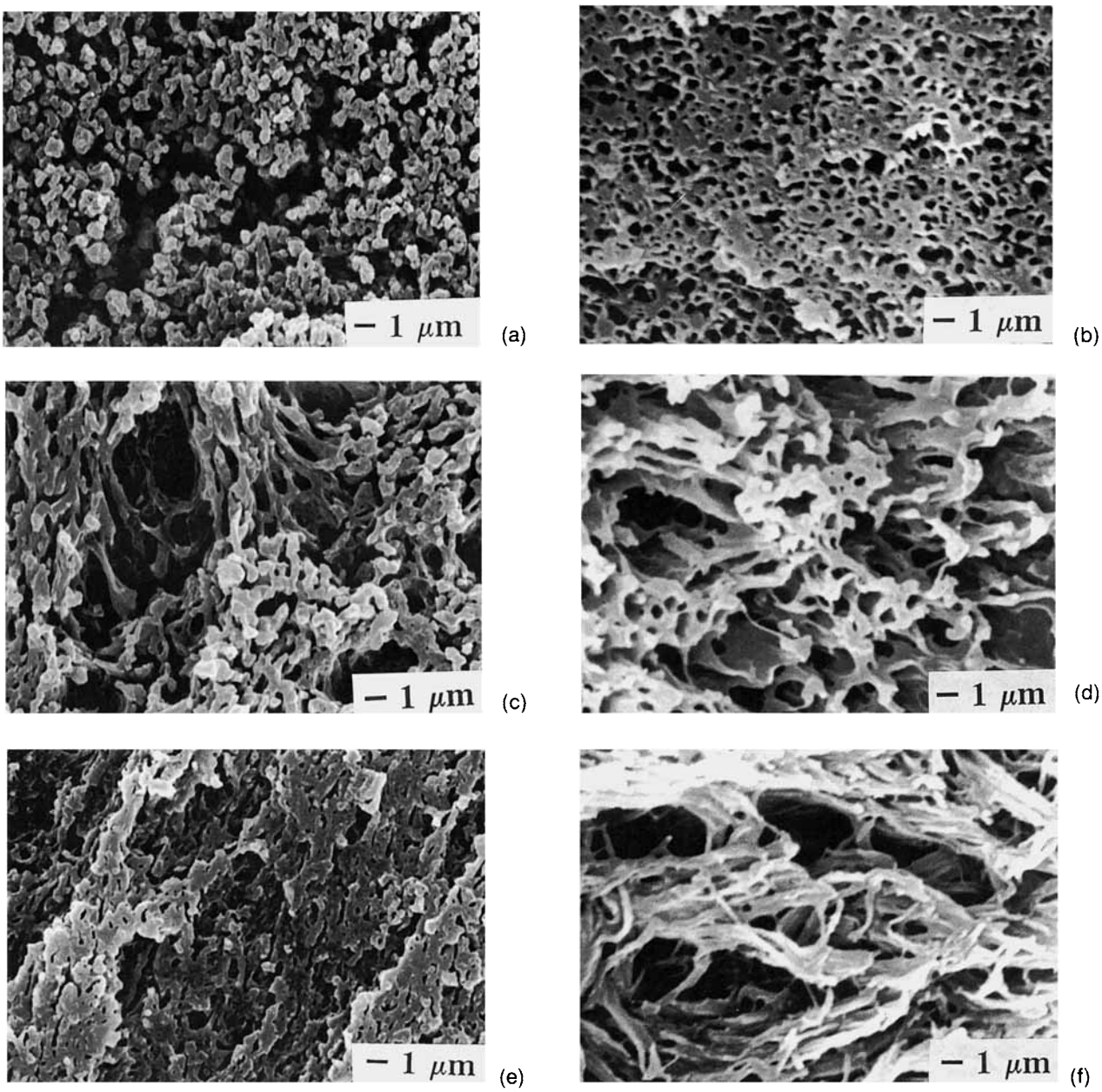

Figure 12 SEM micrographs of (a, c, e) KOH/ethanol-etched and (b, d, f) MEK-etched surfaces of the Izod impact fracture samples for ABS2/PET blends of compositions (a, b) 30/70 (c, d) 50/50, and (e, f) 70/30. The surfaces are perpendicular to the flow direction during molding.

sition as reported by Lombardo et al.,[3] Suarez et al.,[22] and Wu et al.[14] for ABS/PC blends. According to Kolarik,[23] immiscible polymer blends with high interfacial strength exhibit simple additivity of the yield stress, suggesting that the ABS/PET system exhibits some miscibility at the interface.

Falling dart impact traces are shown in Figure 10 for various blends of ABS2/PET. These high-speed force-deflection curves are analogous to the low-speed tensile test data shown in Figure 8 but indicate reduced ductility due to the higher strain rate involved. Under the high-speed impact conditions, the modulus, yield stress, and displacement to break increase in a monotonic fashion when the PET content in the blend in an analogous manner to that was observed for low-speed flexural testing (Fig. 8).

While the notched Izod strength of ABS2/PET passes through a steep maximum centered around

the 50/50 composition, the dart energy shows only a step transition in this region (see Fig. 11). It is not surprising that the Izod and dart energies show such different trends when the differences between the two methods are recognized. For a material to absorb large amounts of impact energy it must be capable of large-scale plastic deformation by shear yielding (or in some cases by crazing, also known as normal yielding).[20] Whether the material in the vicinity of the crack tip experiences yielding or not depends on intrinsic factors such as the magnitude of the yield stress and fracture toughness and on extrinsic factors such as the triaxiality of the stress state (which is controlled by specimen thickness, presence of notches, and testing geometry) and the presence of stress-intensifying flaws or notches. Since the former factors will vary as the blend composition is changed and since the stress state and the presence of notches differ for the two tests,[24,25] quite contrary trends in impact energy can result. For ABS/PC blends, rather complicated and conflicting Izod impact results have been reported.[3,14,22,26] Wu et al.[14] and Suarez et al.[22] observed that the notched Izod strength for ABS/PC blends passes through a minimum [at either 20 (ref. 14) or 50 wt % (ref. 22) PC] as a function of composition while Greco and Dong[26] and Lombardo et al.[3] found that the impact energy either passed through a minimum and a maximum or increased monotonically with rising PC levels. In the present case, the causes of the impact energy variations shown in Figure 11 are also not understood.

The microstructure of the fracture surfaces from impact specimens is shown in Figure 12. By comparison with the freeze-fractured surfaces (Fig. 7), the most extensive plastic deformation in both domains is seen in the 50 wt % PET sample, which absorbed the highest impact energy (700 J/m). The sample with 30 wt % PET shows a reduced level of plastic deformation composition in the ABS phase and has a slightly smaller impact energy (550 J/m). The sample with the lowest toughness (150 J/m) shows little sign of plastic deformation in either phase.

CONCLUSIONS

Novel blends of PET and ABS were prepared by extrusion and injection molding. DSC and DMTA show that blends of ABS with PET consist of four phases—amorphous PET and SAN phases, PBD particles, and small amounts of crystalline PET. There appears to be only limited miscibility of the SAN and PET phases. Transmission electron micrographs reveal that the PBD particles are clustered in the SAN domain and confirm the evidence from scanning electron microscopy that the 50/50 blend has a cocontinuous structure in three dimensions. Some evidence of cocontinuity in the phase structure is seen in blends with 30/70 and 70/30 compositions.

The modulus, yield stress, and breaking stress increased as the wt % PET in the blend was increased. While yield stress and flexural modulus appear predictable by a simple rule of mixtures, the dart impact energy passed through a step transition at 50 wt % PET and the Izod impact energy exhibited a maximum at 50 wt % PET. The degree of toughness of the latter materials was consistent with the extent of plastic deformation on the fracture surface observed by SEM. The high impact behavior of these blends are comparable with PC/ABS blends and may be a replacement for such materials in some applications not limited by the low T_g of the PET phase.

The authors are pleased to acknowledge the assistance of Dr. John Ride (Huntsman) for supply of the ABS and for technical discussions, Mr. Russell Varley (CSIRO) for operation of the DMTA, Mr. Geoff Richardson (ACI) for supply of the PET, and Dr. Ru Wu (CSIRO), Mr. Lawry Mc Carthy (CSIRO), Dr. Michael O'Shea (CRC for Polymer Blends), and Dr. Alastair McKee (CRC for Polymer Blends) for helpful advice.

REFERENCES

1. L. A. Utracki, *Polymer Alloys and Blends: Thermodynamics and Rheology,* Hanser, Munich, 1990.
2. T. A. Callaghan, K. Takakuwa, D. R. Paul, and A. R. Padwa, *Polymer,* **34,** 3797 (1993).
3. B. S. Lombardo, H. Keskkula, and D. R. Paul, *J. Appl. Polym. Sci.,* **54,** 1697 (1994).
4. K. Udipi, Eur. Pat. Appl. EP 0,388,388 (1990) (to Monsanto).
5. M. K. Akkapeddi, T. J. Kraft, and B. Vanbuskirk, U.S. Pat. 5,115,018 A (1992) (to Allied Signal Inc.).
6. R. Binsack, D. Rempel, P. Bier, and C. Lindner, Eur. Pat. EP 82,100,044 (1982) (to Bayer AG).
7. B. Fox, G. Moad G. van Deipen, I. Willing, and W. D. Cook, *Polymer,* to appear.
8. W. D. Cook, G. Moad, B. Fox, G. Van Deipen, T. Zhang, F. Cser, and L. Mc Carthy, to appear.
9. K. H. Illers and H. Breuer, *J. Coll. Sci.,* **18,** 1 (1963).
10. W. N. Kim and C. M. Burns, *Polym. Sci. Eng.,* **28,** 1115 (1988).
11. T. Ricco, A. Pavan, and F. Danusso, *Polymer,* **16,** 685 (1975).

12. C. K. Kim and G. S. Shin, *J. Appl. Polym. Sci.*, **48,** 945 (1993).
13. J. J. Herpels and L. Mascia, *Eur. Polym. J.*, **26,** 997 (1990).
14. J.-S. Wu, S.-C. Shen, and F.-C. Chang, *J. Appl. Polym. Sci.*, **50,** 1379 (1993).
15. J. A. Brydson, *Rubbery Materials and Their Compounds,* Elsevier, 1988, p. 129.
16. M. J. Guest and J. H. Daly, *Eur. Polym. J.*, **26,** 603 (1990).
17. M.-P. Lee, A. Hiltnet, and E. Baer, *Polymer,* **33,** 685 (1992).
18. L. Dong, R. Greco, and G. Orsello, *Polymer,* **34,** 1375 (1993).
19. D. Quintens, G. Groeninckk, M. Guest, and L. Aerts, *Polym. Eng. Sci.*, **30,** 1474 (1990).
20. A. J. Kinloch and R. J. Young, *Fracture Behaviour of Polymers,* Applied Science, London, 1983.
21. G. P. Marshall, *Plast. Rubb. Process. Appl.*, **2,** 169 (1982).
22. H. Suarez, J. W. Barrow, and D. R. Paul, *J. Appl. Polym. Sci.*, **29,** 3253 (1984).
23. J. Kolarik, *Polymer,* **35,** 3631 (1994).
24. R. P. Nimmer, *Polym. Eng. Sci.*, **27,** 263 (1987).
25. C. Cheng, A. Hiltner, E. Baer, P. R. Soskey, and S. G. Myonakis, *J. Appl. Polym. Sci.*, **55,** 1691 (1995).
26. R. Greco and L. Dong, *Macromol. Symp.*, **78,** 141 (1994).

Received January 24, 1996
Accepted 1996